PERGAMON

Chemical Engineering Science 54 (1999) 5887–5899

Chemical Engineering Science

Simulation of the population balances for liquid–liquid systems in a nonideal stirred tank. Part 1 Description and qualitative validation of the model

Ville Alopaeus[a,*], Jukka Koskinen[b], Kari I. Keskinen[b]

[a]*Department of Chemical Technology, Helsinki University of Technology, P.O. Box 6100, 02015 HUT, Finland*
[b]*Neste Oyj Engineering, Porvoo,Finland*

Received 3 August 1998; received in revised form 12 March 1999; accepted 17 March 1999

Abstract

A simulation model has been developed to model drop populations in a stirred tank. A multiblock stirred tank model has been used with the drop population balance equations developed in the literature. The stirred tank is modeled separately so that local turbulent energy dissipation values and fluid flows are used in the drop breakage and coalescence functions. This model has several attractive features, e.g. it can predict the inhomogenity of dispersions and some scale-up phenomena. Because local conditions can be used in the drop rate functions needed in the population balances, it is possible to take these fundamental processes into closer examination. It seems that the parameter values in the drop breakage and coalescence models depend on flow and turbulence averaging for the vessel. This proposes that for "intrinsic" drop breakage and coalescence rates, a multiblock model for the stirred tank is needed in parameter estimation as well. The stirred tank flow model may be obtained from measurements or from computational fluid dynamics simulations in a straightforward manner. © 1999 Elsevier Science Ltd. All rights reserved.

Keywords: Population balances; Liquid–liquid dispersions; Inhomogenity; Computer simulations; Multiblock stirred tank model

1. Introduction

Many chemical processes are based on chemical reactions taking place in stirred tank reactors. Often these are two-phase processes, e.g. solid–liquid, liquid–liquid or gas–liquid. Processes falling into these categories are, for example, crystallization and suspension or emulsion polymerization, and dispersion processes in general. In these processes the particle or drop size distribution, and the heat and mass transfer often affect the product quality.

In two-phase reactors, the mass transfer between phases can be determined from the expressions for mass transfer fluxes, which consist of terms for diffusive and convective fluxes, and the mass transfer area. The determination of drop size distribution and thus the mass transfer area for liquid–liquid dispersions in a stirred tank is the main objective of this article. The drop size distribution may also vary considerably in different regions of the stirred tank. This variation is taken into account in the simulation model presented in this work.

The classical method for determining mass transfer area is based on the correlations for Sauter mean diameter for droplets, a_{32}. These correlations are usually derived for a stationary state, but additional provision is sometimes made to take transients into account. These correlations are averages for the whole vessel only. They do not give any information about the drop size distribution or possible inhomogenities in the stirred tank. In this work, a population balance approach is applied in more complicated and general cases. This approach is applicable in case the drop rate functions are known or can be estimated. The droplets are also assumed to be spherical, if another variable describing the deviation from the spherical shape is not wanted. This additional variable would probably complicate the system too much, with negligible additional value.

The underlying idea in this work is that detailed stirred tank flow data is applied in the model formulation. This flow data can be obtained from a computational fluid dynamics (CFD) model or from flow measurements. From the population balance point of view, the most

* Corresponding author. Fax: 358-9-4512694.
E-mail address: valopaeu@cc.hut.fi (V. Alopaeus)

0009-2509/99/$ - see front matter
PII: S0009-2509(99)00170-0

Nomenclature

a	drop diameter, m
a_{32}	Sauter mean diameter, ($= \Sigma a_i^3/\Sigma a_i^2$), m
a_{max}	maximum drop diameter, m
a_{min}	minimum drop diameter, m
Δa	width of droplet class, m
A_{ij}	area between subregions i and j, m^2
c_f	increase coefficient of surface area
c_m	empirical constant
C_1,C_2, C_3,C_5, C_6	empirical constants
C_4	empirical constant, m^{-2}
D_i	impeller diameter, m
E	surface energy, J
Fr	two-phase Froude number ($= \rho_C N^2 D_i^2/(\Delta\rho\, Hg)$)
$F(a_i, a_j)$	binary coalescence rate between droplets a_i and a_j in unit volume, $m^3\ s^{-1}$
$g(a)$	breakage frequency of drop size a, s^{-1}
$g(a_i,a_j)$	breakage frequency of drop size a_j to a drop f size a_i, s^{-1}
H	tank height, m
$h(a_i,a_j)$	collision frequency between droplets a_i and a_j in unit volume, $m^3\ s^{-1}$
h_1, h_2	film thickness between drops at the beginning and end of drainage
k_1, k_2	constants
k_3, k_4	system parameters ($m^{1.2}\ s^{-0.8}$) and (kg $m^{-1}\ s^{-4}$), respectively
k_5, k_6	system parameters
n	number of drops per unit volume, m^{-3}
n_{in}	drop flow per unit volume into the region of interest, $s^{-1}\ m^{-3}$
n_{out}	drop flow per unit volume out from the region of interest, $s^{-1}\ m^{-3}$
nb	number of subregions (blocks)
nc	number of drop classes
N	impeller speed, s^{-1}
N_P	impeller power number
N_Q	impeller pumping number
N_S	dispersion scale-up number
P	power, W
P_v	droplet volume distribution function
Q	flow rate, $m^3\ s^{-1}$
q	parameter in coalescence efficiency function
$Q_{i,j}$	true flow rate from subregion i to j, $m^3\ s^{-1}$
Q_{ijk}	flow rate of drop class k from subregion i to j, $m^3\ s^{-1}$
$Q^*_{i,j}$	dimensionless flow rate from subregion i to j
r	radial coordinate, m
Re	Reynolds number
t	time, s
t_c	circulation time, s
T	tank diameter, m
Δv	relative velocity between the dispersed and the continuous phase, $m\ s^{-1}$
v_k	relative velocity between droplets and the continuous phase, $m\ s^{-1}$
v_t	droplet terminal velocity, $m\ s^{-1}$
V	total tank volume, m^3
V_i	volume of a subregion i, m^3
$\mathscr{V}_i$	relative volume of a subregion i
$\#(\mathscr{V}_i)$	index number of drop class of characteristic volume $\mathscr{V}_i$
We	Weber number ($= \rho_{dispersion} N^2 D_i^3/\sigma$)
Y_i	number concentration of drop class i, m^{-3}
$Y_{i,j}$	number concentration of drop class i in a subregion j, m^{-3}
$Y_{i,in}$, $Y_{i,out}$	flow of drop class i per unit volume into and out from the region of interest, respectively, $s^{-1}\ m^{-3}$
$Y_{i,j,in}$, $Y_{i,,j,out}$	flow of drop class i per unit volume into and out from the subregion j, respectively, $s^{-1}\ m^{-3}$
z	axial coordinate, m

Greek letters

α	constant
$\beta(a_i,a_j)$	probability that a drop of size a_i is formed when a_j breaks, m^{-1}
β_1	constant
$\beta_r(a_i,a_j)$	relative probability that a drop of size a_i is formed when a_j breaks, m^2
$\Gamma(x)$	gamma function
$\Gamma(a,x)$	incomplete gamma function
$\varepsilon(z,r)$	local turbulent energy dissipation, m^2/s^3
ε_i	average turbulent energy dissipation (per unit mass) in a subregion i, m^2/s^{-3}
ζ	parameter in coalescence efficiency function
η	Kolmogroff length scale, m
κ	viscosity ratio ($= \mu_D/\mu_C$)
λ	eddy size, m
$\lambda(a_i,a_j)$	collision efficiency between droplets a_i and a_j
μ, μ_{disp},	viscosity in general, viscosities of dispersion, dispersed phase and
μ_D, μ_C	continuous phase, respectively, Pa s
$\nu(a)$	number of drops formed when drop of size a is broken
ξ	size ratio between an eddy and a drop
ρ, ρ_{disp},	density in general, densities of dispersion, dispersed phase and
ρ_D, ρ_C	continuous phase, respectively, $kg\ m^{-3}$
σ	interfacial tension, $N\ m^{-1}$
ϕ	volume fraction of dispersed phase
φ	relative turbulent energy dissipation
ω	eddy-drop collision frequency, s^{-1}
ω_v	frequency of velocity fluctuations, s^{-1}

important fluid flow properties are the local turbulent energy dissipations and the local velocities in the case of turbulent flows, and the local shear force rates in laminar flows. Various drop rate functions can then correspondingly be used, possibly with suitable simplifications, with these flow models.

The drop size distribution in two-phase processes is generated by different phenomena, which can be divided into different categories. These are:

- Feed or discharge of droplets in a particular region of the vessel under consideration: Also relative velocities between the continuous phase and the dispersed droplets affect drop size distributions in different parts of the vessel.
- Growth and nucleation of droplets: Droplet growth (or shrinkage) follows from mass transfer into the droplet or out from the droplet, or from those reactions that do not conserve volume. Nucleation follows when the system becomes thermodynamically unstable. This is the case when the Hessian matrix of Gibbs free energy (with respect to mole fractions) is not positive definite in some part of the fluid under consideration (Haase, 1969, p. 69–76; Taylor & Krishna, 1993, pp. 59–66)
- Breakage and coalescence of droplets: These processes are affected by the local mechanical conditions in the dispersion, i.e. turbulent energy dissipation and shear forces. Besides this, by physical properties, i.e. viscosity and density of the phases, interfacial tension, and other interfacial phenomena, such as the surface charge of the droplets.

2. Population balance model

For the chemically equilibrated liquid–liquid dispersion (no growth or shrinkage of droplets due to mass transfer or reaction), the population balance equation for a unit volume is (Valentas & Amundson, 1966; Hsia & Tavlarides, 1980)

$$\begin{aligned}\frac{\mathrm{d}(nA(a))}{\mathrm{d}t} &= n_{\mathrm{in}}A(a) + \int_u^\infty v(a')\beta(a,a')g(a')nA(a')\,\mathrm{d}a' \\ &+ \int_0^{a/\sqrt[3]{2}} \lambda((a^3-a'^3)^{1/3},a')n((a^3-a'^3)^{1/3},a') \\ &nA((a^3-a'^3)^{1/3})nA(a')\,\mathrm{d}a' \\ &- n_{\mathrm{out}}A(a) - g(a)nA(a) - nA(a) \\ &\int_0^\infty \lambda(a,a')h(a,a')nA(a')\,\mathrm{d}a'. \end{aligned} \tag{1}$$

This integro-differential equation can be solved by dividing drop population densities into several discrete classes, and calculating integrals in the above equation numerically. The resulting set of ordinary initial value differential equations can be solved with a standard numerical algorithm. In the discretization, the preceding equation is multiplied by da, and a new working variable is set as

$$Y_i = n_i A(a_i)\,\mathrm{d}a. \tag{2}$$

Y_i is the number concentration of drop class i, and a_i is the characteristic diameter of the class i. The following working equations are then obtained for discrete drop classes:

$$\begin{aligned}\frac{\mathrm{d}Y_i}{\mathrm{d}t} &= Y_{i,\mathrm{in}} + \sum_{j=i+1}^{\mathrm{nc}} v(a_j)\beta(a_i,a_j)g(a_j)Y_j\Delta a \\ &+ \sum_{j=1}^{\#(\mathscr{V}_i/2)} F((a_i^3-a_j^3)^{1/3},a_j)Y_iY_j \\ &- Y_{i,\mathrm{out}} - g(a_i)Y_i - Y_i\sum_{j=1}^{\#(\mathscr{V}_{\mathrm{nc}}-\mathscr{V}_i)} F(a_i,a_j)Y_j, \end{aligned} \tag{3}$$

where $F(a_i, a_j)$ is combined notation for $\lambda(a_i, a_j)h(a_i, a_j)$.

$\#(\mathscr{V}_i/2)$ stands for the index of the class whose characteristic volume is half of the characteristic volume of class i.

$\#(\mathscr{V}_{\mathrm{nc}} - \mathscr{V}_i)$ stands for the index of the class whose characteristic volume is the last class characteristic volume minus the characteristic volume of class i.

The left-hand side stands for time change of number concentration of drops in class i. On the right-hand side, the terms are as follows:

1. number concentration flow into the region where dispersion is assumed homogeneous (convection in),
2. number concentration frequency of droplets born by breakage,
3. number concentration frequency of droplets born by coalescence,
4. number concentration flow from the region of interest (convection out),
5. number concentration frequency of droplets dead by breakage,
6. number concentration frequency of droplets dead by coalescence.

The dispersed phase volume fraction is given as (Hsia & Tavlarides, 1980; Valentas & Amundson, 1966)

$$\phi = n\int_0^\infty \frac{\pi}{6}a^3A(a)\,\mathrm{d}a = \frac{\pi}{6}\sum_{i=1}^{\mathrm{nc}} a_i^3Y_i. \tag{4}$$

For drop size discretization, we need a maximum drop size so that a negligible amount of droplets have a diameter larger than that. Usually maximum drop size for the simulation can be obtained from the following

correlation (Tsouris & Tavlarides, 1994):

$$a_{\max} = c_m We^{-0.6} D_i \left(1 + 2.5\phi \frac{\mu_D + 0.4\mu_C}{\mu_D + \mu_C}\right)^{1.2}, \quad (5)$$

where c_m is a constant, whose value is set at 0.125 or a little larger for further assurance. If larger drops than those predicted by this equation are fed into the vessel, then these must be included in the size range. Minimum drop size is obtained from the Kolmogroff microscale as (Tsouris & Tavlarides, 1994)

$$a_{\min} = \eta = (\mu^3/\rho^3\varepsilon)^{1/4}. \quad (6)$$

Then by assuming that the class width is the same for all classes it is obtained from

$$\Delta a = (a_{\max} - a_{\min})/\mathrm{nc}, \quad (7)$$

and the first characteristic class diameter from

$$a_1 = \Delta a/2 + a_{\min}. \quad (8)$$

No serious error results in the last two equations if the minimum droplet size is set to zero, provided that the discretization interval Δa is larger than the Kolmogroff length scale. In that case, the assumption that the minimum droplet size equals the minimum turbulent eddy size is avoided. This assumption is furthermore criticized, e.g. by Zhou and Kresta (1998).

3. Drop breakage and coalescence rate functions

In the past few decades, the drop rate functions given by Coulaloglou and Tavlarides (1977) seem to have been the most widely used. However, recently some more elaborated functions have been presented. These functions are discussed here to give some insight into the factors affecting the evolution of the drop size distribution. (Tsouris & Tavlarides, 1994; Luo & Svendsen, 1996).

In this work, attention is paid only to turbulent dispersions. The criterion to be satisfied is that the impeller Reynolds number is greater than about 10^3–10^4, that is

$$Re_{\mathrm{imp}} = D_i^2 N\rho/\mu > 10^4. \quad (9)$$

Then the power input into vessel is independent of the impeller Reynolds number, and is given by

$$P = N_P \rho N^3 D_i^5, \quad (10)$$

where N_P is the power number, and its value is usually between 0.3 to 6.0, depending on the impeller type. The power number may, however, assume values not in these limits for more specialized impeller designs. (Brodkey & Hershey, 1988, p. 375; Harnby, Edwards & Nienow, 1992, pp. 137–141, 331–332).

In the turbulent region, the droplet breakage rate is given as

$$g(a_i) = C_1 \frac{\varepsilon^{1/3}}{(1+\phi)a_i^{2/3}} \exp\left(-C_2 \frac{\sigma(1+\phi)^2}{\rho_D \varepsilon^{2/3} a_i^{5/3}}\right). \quad (11)$$

The breakage is assumed to be binary, so that $v(a_i)$ is always 2. Several daughter droplet probability density functions (or "breakage kernels") are used. Among these are the normal distribution and the beta distribution. (Coulaloglou & Tavlarides, 1977; Tsouris & Tavlarides, 1994)

If diameter is the variable that is used in the population balance equations, the beta function can be written as (Bapat, Tavlarides & Smith, 1983)

$$\beta(a_i,a_j) = \frac{90 a_i^2}{a_j^3}\left(\frac{a_i^3}{a_j^3}\right)^2\left(1 - \frac{a_i^3}{a_j^3}\right)^2. \quad (12)$$

If the probability that a droplet is formed is related to the increase of the surface energy in the drop formation, the following equation for probability density is obtained:

$$\beta(a_i,a_j) = \frac{E_{\min} + (E_{\max} - E(a_i))}{\int_0^{a_j} (E_{\min} + (E_{\max} - E(a_i)))\,\mathrm{d}a'}, \quad (13)$$

where $E = \pi a^2 \sigma$ is the surface energy of the droplet (Tsouris & Tavlarides, 1994)

If the scaling in the denominator is done separately (see discussion below), the above equation can be put into the following discrete form:

$$\beta_r(a_i,a_j) = a_{\min}^2 + (\sqrt[3]{2} - 1)a_j^2 - a_i^2 + (a_j^3 - a_{\min}^3)^{2/3} - (a_j^3 - a_i^3)^{2/3}. \quad (14)$$

It can be seen that these functions are completely different in shape, the beta function giving the maximum at the equal volume breakage, while the probability based on energetic aspects gives the minimum at the equal volume breakage. Minimum drop size can again be set equal to the Kolmogroff length scale.

The following equation for drop breakage does not need an additional probability distribution or adjustable parameters.

$$g(a_i,a_j) = k_1\beta_1(1-\phi)\left(\frac{\varepsilon}{a_j^2}\right)^{1/3} \int_{\xi_{\min}}^{1} \frac{(1+\xi)^2}{\xi^{11/3}} \exp\left(-\frac{12 c_f \sigma}{\beta_1 \rho_C \varepsilon^{2/3} a_j^{5/3} \xi^{11/3}}\right) \mathrm{d}\xi. \quad (15)$$

This gives the breakage rate of a drop of size a_j to two drops, one of size a_i and the other correspondingly of size $(a_j^3 - a_i^3)^{1/3}$, so that the probability distribution is implicitly built into the function. The physical interpretation for ξ is the size ratio between an eddy and a drop. The following equations give us the unknown variable and

constants.

$$c_f = \frac{a_i^2}{a_j^2} + \left(1 - \frac{a_i^3}{a_j^3}\right)^{2/3} - 1, \tag{16}$$

$$k_1 = \frac{15\pi^{1/3}}{8 \times 2^{2/3}\Gamma(1/3)}\beta_1^{1/2}, \tag{17}$$

$$\beta_1 = \frac{8\Gamma(1/3)}{5\pi}\alpha. \tag{18}$$

α is a parameter, which comes from the relation for a turbulent energy spectrum

$$E(k) = \alpha\varepsilon^{2/3}k^{-5/3}. \tag{19}$$

Here $\alpha = 1.5$ is used, so that $\beta_1 \approx 2.0466$ and $k_1 \approx 0.9238$ (Luo & Svendsen, 1996). The above integral equation can be calculated by using incomplete gamma functions in the following manner:

$$g(a_i, a_j) = \frac{-3k_1\beta_1(1-\phi)}{11b^{8/11}}\left(\frac{\varepsilon}{a_j^2}\right)^{1/3} \{\Gamma(8/11, t_m) - \Gamma(8/11, b) + 2b^{3/11}(\Gamma(5/11, t_m) - \Gamma(5/11, b)) + b^{6/11}(\Gamma(2/11, t_m) - \Gamma(2/11, b)\} \tag{20}$$

where

$$b = \frac{12c_f\sigma}{\beta_1\rho_C\varepsilon^{2/3}a_j^{5/3}} \quad \text{and} \quad t_m = b(\eta/a_j)^{-11/3}.$$

Numerical procedures for calculating incomplete gamma functions are given in literature (Press, Teukolsky, Vetterling & Flannery, 1993, pp. 209–213).

The population balance equations must be slightly modified with the above breakage function. This is because the above function gives both breakage rates and the daughter droplet size distributions. The term $\beta(a, a')g(a')$ is combined into $g(a, a')$, and the droplet disappearance by breakage term must be obtained by integrating birth by breakage rates over all possible daughter drop sizes. The breakage rate is modified as follows:

$$g(a) \text{ is replaced by } \int_0^a \frac{g(a', a)}{2a}\mathrm{d}a'. \tag{21}$$

This integral must be calculated numerically in the discretized population balance model.

A quite different mechanism for drop breakage has been proposed by Wichterle (1995). In that work it has been assumed that drop breakage depends on the laminar boundary layer at the tip of the impeller, even in turbulent dispersions. This approach is then shown to give good results, at least if stationary drop sizes are considered. However, no drop breakage frequency function was introduced in that work. Similar extensions to the breakage models are proposed by Kumar, Kumar and Gandhi (1991). They proposed that drop breakage occurs through three mechanisms, turbulent breakup, elongation flow breakup in the accelerating flow along the impeller length, and shear mechanism in the boundary layer at the impeller. These mechanisms then operate simultaneously, composing the total breakage rate. However, no parameters needed for the population balance approach are presented.

The binary droplet coalescence rate is given by Coulaloglou and Tavlarides (1977). The original equation seems to be slightly erroneous, and the term $(a_i^2 + a_j^2)$ is replaced by $(a_i + a_j)^2$. This correction is done by several authors in the past (Bapat, Tavlarides & Smith 1983; Hsia & Tavlarides, 1983; Tsouris & Tavlarides, 1994).

$$F(a_i, a_j) = C_3\frac{\varepsilon^{1/3}}{1+\phi}(a_i + a_j)^2(a_i^{2/3} + a_j^{2/3})^{1/2} \exp\left(-C_4\frac{\mu_C\rho_C\varepsilon}{\sigma^2(1+\phi)^3}\left(\frac{a_i a_j}{a_i + a_j}\right)^4\right). \tag{22}$$

In the above equations, $C_1 - C_4$ are empirical constants, and they are postulated to be universal. Some of the values used by different investigators are shown in Table 1.

A different equation is given by Tsouris and Tavlarides (1994), with only one adjustable parameter. Their equations can be put in the following form: The collision frequency is

$$h(a_i, a_j) = \frac{\pi\alpha^{1/2}}{\sqrt[3]{2}}\varepsilon^{1/3}(a_i + a_j)^2(a_i^{2/3} + a_j^{2/3})^{1/2}. \tag{23}$$

The parameter α is the same as in Eq. (19). It is retained here because of its fundamental background in the turbulence theory. The collision efficiency is

$$\lambda(a_i, a_j) = \exp\left(-\frac{6\pi\mu_C C_5\zeta \cdot 31.25ND_i}{\rho_C\varepsilon_{\text{disp}}^{2/3}(a_i + a_j)^{2/3}(T^2H)^{1/3}}\right), \tag{24}$$

with

$$\zeta = 1.872\ln\left(\frac{h_1^{1/2} + 1.378q}{h_2^{1/2} + 1.378q}\right) + 0.127\ln\left(\frac{h_1^{1/2} + 0.312q}{h_2^{1/2} + 0.312q}\right) \tag{25}$$

Table 1
Numerical values for the empirical constants in the drop rate functions of Coulaloglou and Tavlarides (1977) (our Eqs. (11) and (22)) according to Bapat and Tavlarides (1985)

Proposed by/year	C_1	C_2	C_3	$C_4(m^2)$
Hsia (1981)	0.01031	0.06354	4.5×10^{-4}	1.891×10^{13}
Coulaloglou (1975)	0.00487	0.0552	2.17×10^{-4}	2.28×10^{13}
Ross et al. (1978)	0.00487	0.08	2.17×10^{-4}	3.0×10^{12}
Bapat and Tavlarides (1985)	0.00481	0.08	1.9×10^{-3}	2.0×10^{12}

and

$$q = \frac{1}{\kappa}\left(\frac{a_i a_j}{2(a_i + a_j)}\right)^{1/2}. \tag{26}$$

This collision efficiency can be simplified to some extent. First we use assumptions given by Tsouris and Tavlarides ($h_2^{1/2} \ll 0.312q$, and $h_1 = 0.1(\kappa q)^2$), and then approximate the logarithmic term numerically. Finally, we end up with

$$\lambda(a_i, a_j) = (0.26144/\kappa + 1)^{p1}$$

$$P1 = \left(-\frac{C_6 \mu_C}{\rho_C N_p^{1/3} \varepsilon_{\text{disp}}^{1/3} (a_i + a_j)^{2/3} D_i^{2/3}}\right), \tag{27}$$

where $C_6 \approx 1712 C_5$. It is interesting to note that this collision efficiency depends on the impeller diameter as well as the impeller power number. The impeller dependent part in the collision efficiency equation comes from the equation for frequency of velocity fluctuations in a stirred tank, as given by Schwartzberg and Treybal (1968):

$$\omega_v = \frac{31.25 N D_i^2}{(T^2 H)^{1/3}}. \tag{28}$$

This is taken as a reciprocal of the contact time between colliding droplets.

These functions give the collision frequency several orders of magnitude greater than those of Coulaloglou and Tavlarides (1977). Eq. (27) also predicts that coalescence efficiency increases with increasing drop diameter, which is completely opposite to that of Eq. (22). In all these drop rate equations, drops are assumed to behave like gas molecules. This is quite a vague assumption, and is, in fact, in conflict with the drainage models used in the coalescence efficiency equation. A remedy to this should be obtained in the future, as direct numerical simulations of turbulent dispersions become increasingly precise, especially in the case of two-phase systems.

One possible estimate for the drop Sauter mean diameter can be obtained by assuming only one drop class, and setting coalescence and breakage rates as equal:

$$Y \cdot F(a, a) = g(a). \tag{29}$$

Inserting $Y = 6\phi/\pi a^3$ and the drop rate functions of Coulaloglou and Tavlarides (1977), we get, after some algebraic manipulation

$$\ln\left(10.8038\phi \frac{C_3}{C_1}\right) = C_4 \frac{\mu_C \rho_C \varepsilon}{\sigma^2 (1 + \phi)^3}\left(\frac{a}{2}\right)^4 - C_2 \frac{\sigma(1 + \phi)^2}{\rho_D \varepsilon^{2/3} a^{5/3}}. \tag{30}$$

This equation can be solved numerically for a to get an estimate for the Sauter mean diameter. This estimate is quite crude, but still a quite reasonable initial approximation. This approach has a more fundamental background than the commonly used Sauter mean diameter correlations, where diameter is correlated from the Weber number. Hence, it can be assumed that better results are obtained by this method than the classical method, provided that the three parameters, C_3/C_1,C_4, and C_2 are correct. With this approach, some of the deficiencies in the Sauter mean diameter correlations, as shown by Pacek, Man and Nienow (1998), are overcome.

4. Implementation aspects

There are a few aspects to be considered when the discrete model is coded for an equation solver. Firstly, the probability density function $\beta(a_i,a_j)$ must be scaled so that volume is conserved in drop breakage. In fact, mass is the correct property to conserve, but since the system is assumed to be in chemical equilibrium and incompressible, this is equivalent to saying that volume is conserved. This conservation is most easily done by setting the total volume of droplets born by breakage as equal to the total volume of the droplets dead by breakage. Then no scaling is needed in the probability density function.

The other point is that $\#(\nu_i/2)$ and $\#(\nu_{nc} - \nu_i)$ are not necessarily integer numbers. In fact, if the drops are divided into diameter classes of equal length, each specified by a characteristic diameter, then after a two-drop collision the resulting drop diameter is never exactly equal to any of the characteristic drop class diameters, according to the celebrated Fermat's theorem. The remedy for this problem is the following. The coalescence functions are calculated separately over all possible coalescence pairs. When two droplets coalesce, the resulting droplet is divided into the two nearest drop classes according to the third moment of the diameters. This division is made so that both the number of the droplets and their volume is conserved. If the resulting droplet has a diameter greater than the largest droplet class, then the actual volume of that droplet is put into the largest class, so that a number of droplets greater than one is formed for that class. This should, however, be avoided as far as possible by selecting a large enough diameter for the largest droplet class, so that negligible amounts of droplets larger than that are formed. Care must also be taken to avoid counting collisions between two equal drop sizes twice.

Here the implementation is made so that arbitrary discretization can be used if wanted. Selective refinement during simulation can also be made. This article, however, focuses on nonuniform features of dispersion in a stirred tank, so that the accuracy of the solution is obtained by choosing a large enough number of drop size discretization classes. These discretization aspects have been discussed further by Kumar and Ramkrishna (1996a,b)

5. Stirred tank model

The breakage and coalescence phenomena are affected primarily by local turbulence dissipation. Turbulence is not homogenous in a stirred tank, so that near the impeller turbulence is several orders of magnitude greater than near the wall, or at the surface of the dispersion or at the bottom of the tank. The result is that breakage of the droplets especially occurs almost exclusively near the impeller. On the other hand, the impeller pumps dispersion all over the tank. Inhomogenities in the tank will result if circulation in the tank is not sufficiently faster than the breakage and coalescence phenomena. In the literature, a plug flow model is used to take this inhomogenity and circulation into account (Park & Blair, 1975). A new flow model implementation based on the known flow fields is used in this work. These flow fields have been presented, for example, by Bourne and Yu (1994)

In CFD simulations the stirred tank is usually divided into tens of thousands control volumes, and in some cases, even up to a million. A complete CFD model with population balances calculated in each cell is thus considered too complicated for a full population balance. Thus we average the results of these complicated models and use a simplified flow model that includes only a limited number of control volumes. Simplification can be made in a straightforward manner by averaging from the full-scale CFD calculations, and various degrees of simplification can be made easily. It has also been assumed that a simplified model can reveal all the underlying phenomena regarding non-idealities in a stirred tank. A similar approach in using CFD results has been recently adopted by Maggioris, Goulas, Alexopoulos, Chatsi and Kiparissides (1998), who used a two block flow model in the population balances.

The stirred tank is divided into 11 subregions as shown in Fig. 1, where one half of the tank is shown. Symmetry around the impeller axis is assumed.

The local turbulence dissipations in the different subregions, and flows between the subregions were obtained from the work of Bourne and Yu (1994). Here each subregion is assumed to be completely mixed and homogenous, so that volume averaging must be done in the following way for each region.

The energy dissipation is

$$\varepsilon_i = \frac{\int_{r_0}^{r_1}\int_{z_0}^{z_1} 2\pi\varepsilon(z,r)\,\mathrm{d}z\,\mathrm{d}r}{V_i}, \tag{31}$$

where the volume of the subregion is

$$V_i = \int_{r_0}^{r_1}\int_{z_0}^{z_1} 2\pi r\,\mathrm{d}z\,\mathrm{d}r. \tag{32}$$

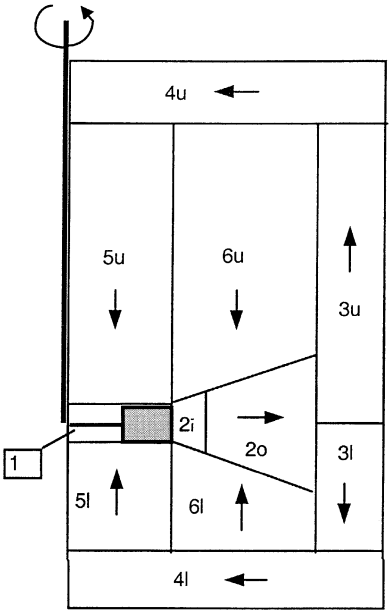

Fig. 1. Subregions chosen for simulation in a stirred tank.

Average turbulent energy dissipation in the whole vessel is obtained from

$$\varepsilon_{\mathrm{ave}} = N_P D_i^5 N^3 / V. \tag{33}$$

It is assumed that all energy input to the vessel is dissipated by turbulent mechanisms.

The volume averaged relative turbulent dissipation is defined as

$$\phi = \varepsilon/\varepsilon_{\mathrm{ave}}. \tag{34}$$

Relative turbulent dissipations and corresponding subregion volumes are given in Table 2. Scaling is made here so that

$$\Sigma \mathscr{V}_i = 1 \tag{35}$$

$$\Sigma \mathscr{V}_i \varphi_i = 1. \tag{36}$$

Internal flow patterns are needed for droplet convection between the subregions. Dimensionless flow values (pumping numbers between the subregions) are here defined as

$$Q^*_{i,j} = Q/(ND_i^3). \tag{37}$$

These values are given in Table 3.

These values are adapted from the velocities presented by Bourne and Yu (1994), by taking their equation for radial flow rate in discharge:

$$N_Q = Q^*_{1,2i} = Q/(ND_i^3) = 2.33(r/D_i) - 0.379 \tag{38}$$

Table 2
Relative turbulent dissipations and volumes of different regions

Subregion	ε_i	φ_i
1	0.0073	34
2i	0.0093	12
2o	0.0755	4.6
3u	0.2052	0.56
3l	0.0846	0.56
4u	0.0950	0.073
4l	0.1000	0.073
5u	0.0584	1.1
5l	0.0219	1.1
6u	0.2603	0.092
6l	0.0825	0.092

Table 3
Dimensionless flow values between the subregions

Flow	Q^*
1 → 2i	0.7860
2i → 2o	1.1006
2o → 3u	1.3641
2o → 3l	1.0492
3u → 4u	1.3641
3l → 4l	1.0492
4u → 5u	0.4443
4l → 5l	0.3417
4u → 6u	0.9198
4l → 6l	0.7075
6u → 2i	0.1778
6l → 2i	0.1368
6u → 2o	0.7420
6l → 2o	0.5707
5u → 1	0.4443
5l → 1	0.3417

as a basis as the flow values are made consistent. The exact positions of the subregions are, in fact, not important provided that the turbulent dissipation and flow rates are correct. These turbulent dissipation and flow values are quite comparable to our own CFD calculations done with the CFX4 code, using 55,620 control volumes. Further refinement of these values and the methodology to choose the appropriate volumes are left for the future.

Now the convection terms in the discretized population balance equation (3) can be calculated as

$$Y_{i,j,\text{in}} = \sum_{k=1}^{\text{nb}} \frac{Q_{kj} Y_{i,k}}{V_j} \quad \text{and} \quad Y_{i,j,\text{out}} = \sum_{k=1}^{\text{nb}} \frac{Q_{jk} Y_{i,j}}{V_j}, \tag{39}$$

where double indexed $Y_{i,j}$ is the number concentration of drop size i in block j, and the third index $_{\text{in}}$ or $_{\text{out}}$ again stands for convection speed in or out. Additional terms for convection into the vessel and out from the vessel must be added for a continuous flow operation.

If the relative velocity between the drop phase and the dispersed phase is taken into account, an additional term must be added to the flow variable between the blocks as

$$Q_{ijk} = Q_{ij} + \Delta v_k A_{ij}, \tag{40}$$

where Δv_k is the relative velocity between the drop phase and the dispersed phase for drop class k,A_{ij} is the area between blocks i and j.

If no drop separation due to a gravitational or a centrifugal field is assumed, then ϕ is constant in each block. Otherwise ϕ varies from block to block, and the settling and centrifugal characteristics of the vessel are also modeled. For population balance simulations of liquid–liquid systems with comparable densities of the two phases, the relative velocity between the phases can be neglected in most cases.

The relative velocity between the phases can be calculated from terminal velocity and a correction for high holdup (Coulson & Richardson, 1991, p. 604). Terminal velocity can be calculated from a modified Stokes law if droplets are small, rigid and spherical, and the drops are assumed to accelerate to terminal velocity instantaneously. Stokes law is modified to take centrifugal forces into account as

$$v_t = g' a \Delta\rho / 18\mu, \tag{41}$$

where g' is the total acceleration due to gravity and centripetal acceleration. This equation is valid only for a drop Reynolds number less than about two.

Stokes law can be augmented to take circulation inside droplets into account by multiplying the rigid drop terminal velocity value by $(1 + \kappa)/(2/3 + \kappa)$, where κ is the viscosity ratio between the dispersed and the continuous phase. (Clift, Grace & Weber, 1978, pp. 33–35)

Apparent dispersion viscosity and density for liquid–liquid systems is calculated with the following equations:

$$\mu_{\text{disp}} = \frac{\mu_C}{1-\phi}\left(1 + 1.5\phi\frac{\mu_D}{\mu_C + \mu_D}\right), \tag{42}$$

$$\rho_{\text{disp}} = \phi\rho_D + (1-\phi)\rho_C. \tag{43}$$

These values are used whenever properties of the dispersion as a whole are needed, like in power input and impeller Reynolds number calculations and in Kolmogroff length scales (Vermeulen, Williams & Langlois, 1955; Perry & Green, 1997, pp. 15–24).

It has been proposed that the droplet sizes, and possibly the size distribution, has a significant influence on dispersion viscosity and other rheological properties. Fine emulsions are shown to have larger viscosities than coarse emulsions (Pal, 1996). The range of drop sizes in that work are below those usually found in stirred tanks, and no quantitative equation is given for drop size effect.

With the apparent dispersion viscosity and density, we can write an equation for the turbulence damping effect on turbulent energy dissipation. For turbulent energy dissipation in dispersions, we adopt the following equation (Doulah, 1975):

$$\varepsilon_{\text{disp}} = \varepsilon_C \left(\frac{\mu_C \rho_{\text{disp}}}{\mu_{\text{disp}} \rho_C} \right)^3. \tag{44}$$

Inserting the above values for apparent dispersion viscosity and density, we obtain

$$\varepsilon_{\text{disp}} = \varepsilon_C \left(\frac{(1-\phi)(\phi\rho_D/\rho_C + (1-\phi))}{1 + 1.5\phi \dfrac{\mu_D}{\mu_D + \mu_C}} \right)^3. \tag{45}$$

Dispersion inhomogenities are often disregarded when drop size distributions are simulated. Experimentally, these inhomogenities are reported to be in the range 1.2–29%, depending on the physical properties and the dispersed phase volume fraction (Chatzi & Kiparissides, 1995). These experiments are, however, usually made in small-scale tanks, which are usually about one liter in volume. Furthermore, to try to avoid inhomogenities in these experiments, an impeller larger in diameter than the usual $D_i = T/3$ may be used.

Dispersion inhomogenity in scaleup can be studied in the following way. First we define a dimensionless number describing the proportion of average circulation time to the average time interval of breakages in the vessel. Here this number is called the "dispersion scale-up number". It describes the relative susceptibility to inhomogenity in a vessel. It is defined here as

$$N_S = t_c g(a_{32}), \tag{46}$$

where a_{32} is the Sauter mean diameter. The circulation time for stirred tanks agitated with the Rushton turbine is given by Holmes, Voncken and Dekker (1964):

$$t_c = k_2 N^{-1} (T/D_i)^2. \tag{47}$$

If the breakage function is as given by Coulaloglou and Tavlarides (1977), and the Sauter mean diameter is assumed to be $a_{32} \propto (P/V)^{-0.4}$, as most of the correlations propose, the dispersion scale-up number can be put into the following form:

$$N_S = k_3 (T/D_i)^2 D_i^{1.2} N^{0.8} = \frac{k_4 (P/V)^{3/5}}{N}. \tag{48}$$

The second equality assumes geometric similarity during scaleup (constant T/D_i value). k_3 and k_4 are parameters, which depend on universal constants in the breakage function, the power number of the impeller, physical properties, dispersed phase volume fraction, but not on the impeller speed or diameter. k_4 also depends on geometrical ratios of the vessel.

It can thus be seen that the dispersion scaleup number increases as impeller speed decreases with constant power/volume ratio and geometric similarity, as usually is the case in dispersion process scale-up. This proposes that inhomogenities increase in larger vessels.

6. Simulation results

Physical properties are taken from an industrially important synthesis, where two immiscible liquid phases are stirred in a semibatch reactor. Two cases are studied: The first corresponds to the situation at the beginning of the synthesis and the second at the end. The corresponding physical properties are:

System 1, *at the beginning of the synthesis*:

$\mu_D = 0.00067$ Pas, $\mu_C = 0.00126$ Pas, $\rho_D = 805$ kg m^{-3},

$\rho_C = 1064$ kg m^{-3}, $\sigma = 0.024$ N m^{-1}.

System 2, *at the end of the synthesis*:

$\mu_D = 0.0205$ Pas, $\mu_C = 0.002$ Pas, $\rho_D = 923$ kg m^{-3},

$\rho_C = 1193$ kg m^{-3}, $\sigma = 0.002$ N m^{-1}.

Vessel specifications for these simulations are:

$N_P = 5.0$, $T = 3.0$ m, $H = 3.0$ m

$D_i = 1.0$ m, $\phi = 0.4$.

A quite significant feature for this system is the relatively low interfacial tension at the end of the synthesis. Along with the high dispersed phase holdup fraction, this results in a system where inhomogenities in the vessel are likely to occur.

For illustration, the drop rate parameters of Hsia (1981) are chosen, and the beta distribution is used as the breakage kernel.

Firstly, the effect of drop diameter discretization is studied by simulating the two systems with different numbers of drop classes. Two steady states with different impeller speeds ($N = 0.5$ and 1.0 s^{-1}) are studied for both systems, and one transient where impeller speed is increased from 0.5 to 1.0 s^{-1}. Transient values are obtained at the moment when the dispersion has been agitated ten seconds with the higher impeller speed. Relative errors with different numbers of drop classes are shown in Fig. 2. Since an analytical solution to the population balance equation is not possible except in some special cases, values are compared to those obtained in simulations with a maximum reasonable number of drop classes, or a number of classes beyond which no change is found as the number of classes is further increased.

It can be seen that about fifteen drop classes give quite reasonable results. In almost all cases, the error of both

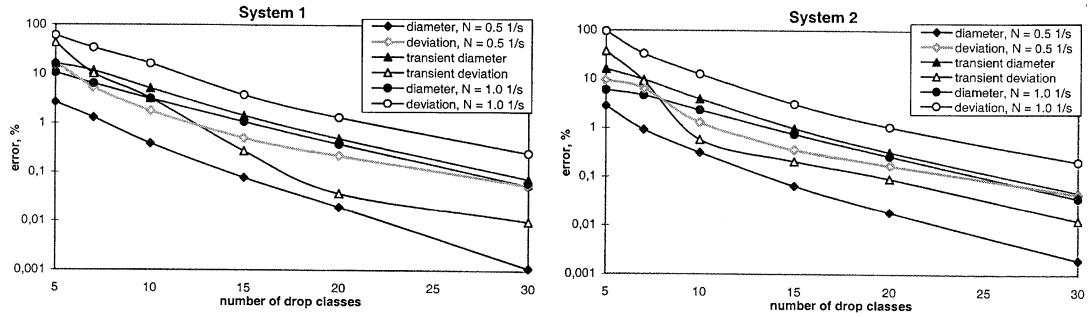

Fig. 2. Relative errors with different numbers of drop classes.

the Sauter mean diameter and the standard deviation is less than a few percent, the error in the standard deviation for the higher impeller speed being slightly higher. For a steady-state solution, slightly fewer classes are needed than for a transient solution. Maximum and minimum drop class sizes must also be chosen so that there are not many classes with negligible amount of drops within. This effect can be seen from Fig. 3, where drop classes are kept constant as impeller speed is increased. This results in more useless drop classes at the upper end of the discretization interval, and a slightly larger error.

In Fig. 3, two transients are shown, where an emulsion with system 2 properties is initially stabilized by mixing it for a long time at impeller speeds $N = 0.5\ s^{-1}$ and $N = 1.0\ s^{-1}$, respectively. At time $t = 0$ impeller speed is either increased from 0.5 to 1.0 s^{-1} or decreased from 1.0 to 0.5 s^{-1}. 15 drop classes are used. Only one volume block is used, i.e. the vessel is assumed as homogeneous. When N is increased, the population curve moves from the higher diameters to the lower ones, and when decreased, in the opposite direction.

It can be seen that the transient is much slower if the impeller speed is decreased compared to the case where it is increased. The drop population is quite close to steady state after 60 s if impeller speed is increased, and after about 2 min, if decreased.

The same transients are then simulated with the multiblock model. In these transient calculations, it is assumed that the flow patterns in the multiblock model are established immediately after the step change in the impeller speed. Fig. 4 shows transients for increasing (on the left) and decreasing (on the right) impeller speeds. Sauter mean diameters in three blocks and the overall Sauter mean diameter in the vessel are plotted. Block names are shown in Fig. 3. Corresponding steady-state populations are shown in Fig. 5.

From Figs. 3–5, it can be seen that the discretization affects populations to some extent, although the average energy dissipation is the same. The standard deviation of the population especially is much larger in the multiblock model, about twice in these cases. The difference in the Sauter mean diameter is, however, not so great at the steady states, but during transients some deviations can be seen, as is shown in Fig. 6. The multiblock model predicts slower responses than the single block model.

7. Conclusion and future work

The population balance approach is capable of describing various phenomena in liquid–liquid systems. However, by assuming a stirred tank to be homogeneous, a serious error might be introduced, since turbulent energy dissipation is several orders of magnitude greater near the impeller than far from it. This error can appear in both giving erroneous values of drop sizes in different parts of the vessel due to inhomogenity, but also because fundamental breakage and coalescence processes are different if the vessel is examined more locally, leading to erroneous overall drop mean diameter. The differences in the drop populations revealed by the simulations of different flow models suggests that the drop rate parameters should be fitted with a more realistic (i.e. multiblock) model. Other drop breakage models can also be introduced at that point. In a single block model serious errors may be introduced if the drop populations are measured at one point in a vessel only. Thus, the multiblock model may also be used to give better parameter values.

The stirred tank model presented here is quite general, and it is very flexible in describing inhomogenity in a stirred tank. This model can also predict scaleup effects in dispersions. These effects arise because equal power input per volume cannot usually be sustained when a laboratory scale reaction is scaled up to a pilot or a full-scale process, resulting in increased drop size and mass transfer resistance. Furthermore, even if power per volume is kept constant, flow patterns change in a scaleup.

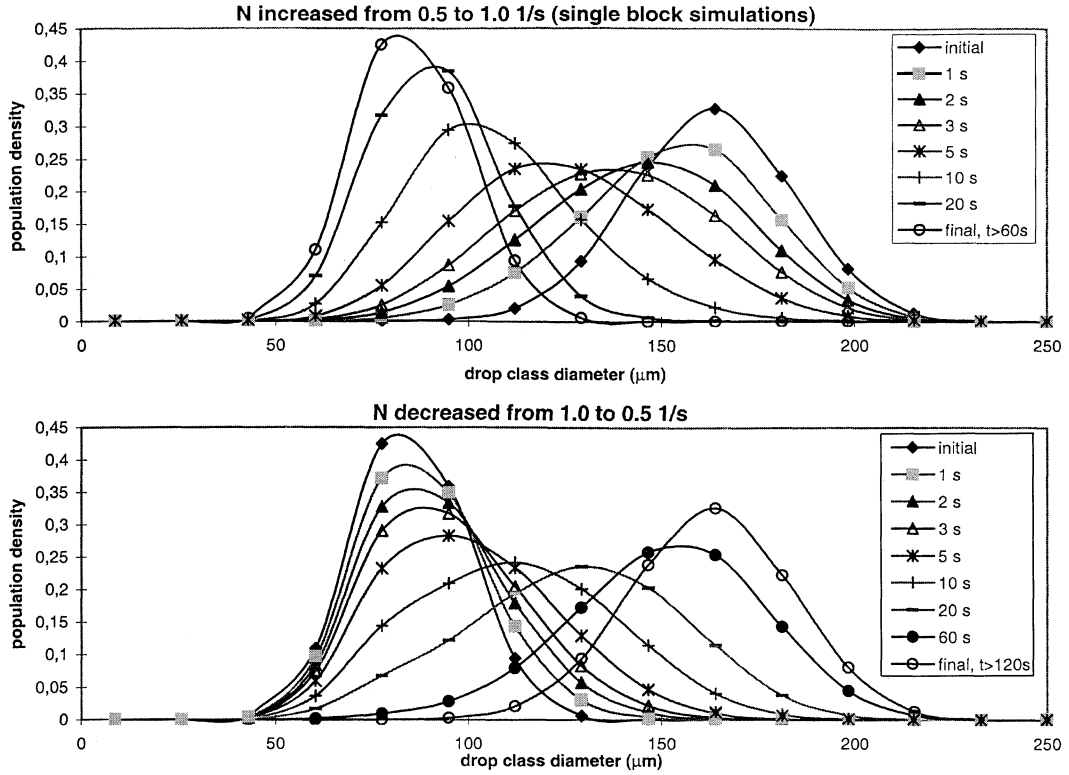

Fig. 3. Transient response as impeller speed is changed.

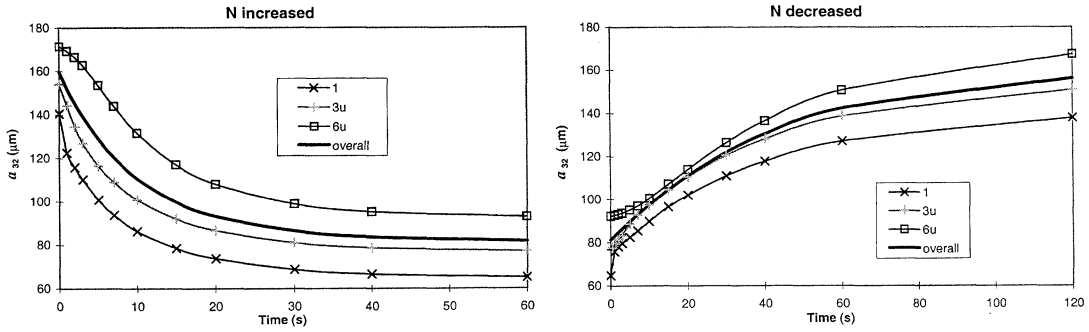

Fig. 4. Transient Sauter mean diameters in a multiblock system.

A stirred tank population balance simulation approach can reduce the uncertainty experienced in this process.

This work is continuing with drop population measurements and parameter estimation with a multi-block model. This is necessary to correctly describe the various phenomena, and it is thus hoped to obtain more universal drop rate parameters this way, since one further phenomenon, i.e. the combined effect of flow patterns

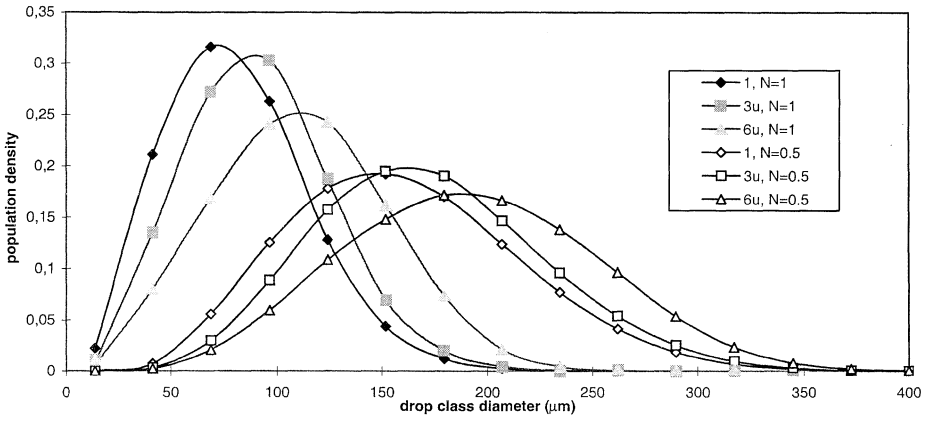

Fig. 5. Steady-state population distributions with two impeller speeds. Population densities are shown in three different blocks of the vessel.

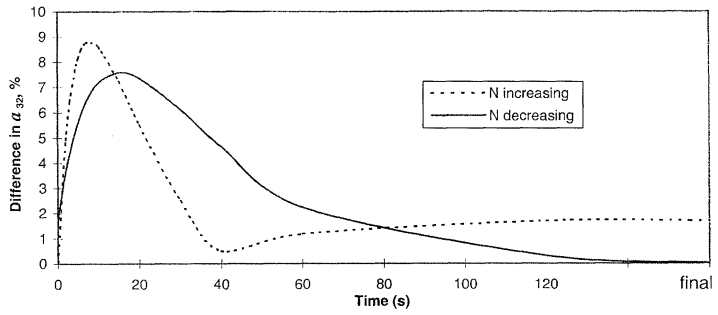

Fig. 6. Differences in Sauter mean diameter between the multiblock and the single block models.

and turbulence inhomogenity, can be excluded from the "intrinsic" population balance simulation. In the future, this model is to be used in connection with CFD reactor simulations, by using the turbulence and fluid flow values obtained from the CFD model, and also for the way that this multiblock population balance model gives the drop size information to the CFD reactor simulator for mass transfer and two-phase flow calculations. Settling characteristics may also be introduced, so that inhomogenity in the phase fractions in different parts of a vessel is described correctly. Furthermore, this stirred tank model may also be used with population balance equations and rate functions of other processes, such as precipitation or crystallization.

Acknowledgements

Financial support from Neste Oy Foundation and the Brite Euram program, contract number BRPR-CT96-0185, are gratefully acknowledged.

References

Bapat, P. M., & Tavlarides, L. L. (1985). Mass transfer in a liquid-liquid CFSTR. *A.I.Ch.E. Journal*, *31*, 659–666.

Bapat, P. M., Tavlarides, L. L., & Smith, G. W. (1983). Monte Carlo simulation of mass transfer in liquid-liquid dispersions. *Chemical Engineering Science*, *38*, 2003–2013.

Bourne, J. R., & Yu, S. (1994). Investigation of micromixing in stirred tank reactors using parallel reactions. *Industrial and Engineering Chemistry Research*, *33*, 41–55.

Brodkey, R. S., & Hershey, H. C. (1988). *Transport phenomena, a unified approach*. New York: McGraw-Hill.

Chatzi, E. G., & Kiparissides, C. (1995). Steady-state drop-size distributions in high holdup fraction dispersion systems. *A.I.Ch.E. Journal*, *41*, 1640–1652.

Clift, R., Grace, J. R., & Weber, M. E. (1978). *Bubbles, drops, and particles*. New York: Academic Press.

Coulaloglou, C. A., & Tavlarides, L. L. (1977). Description of interaction processes in agitated liquid-liquid dispersions. *Chemical Engineering Science*, *32*, 1289–1297.

Coulson, J.M., & Richardson, J.F. (1991). *Chemical engineering*, vol. 2 (4th ed.). Oxford: Pergamon Press.

Doulah, M. S. (1975). An effect of hold-up on drop sizes in liquid-liquid dispersions. *Industrial and Engineering Chemistry, Fundamentals*, *14*, 137–138.

Haase, R. (1969). Thermodynamics of irreversible processes. Reading, MA: Addison-Wesley.

Harnby, N., Edwards, M.F., & Nienow, A.W. (1992). *Mixing in the process industries* (2nd ed.). London: Butterworth-Heinemann.

Holmes, D. B., Voncken, R. M., & Dekker, J. A. (1964). Fluid flow in turbine-stirred, baffled tanks-I, circulation time. *Chemical Engineering Science*, *19*, 201–208.

Hsia, M. A., & Tavlarides, L. L. (1980). A simulation model for homogeneous dispersion in stirred tanks. *Chemical Engineering Journal*, *20*, 225–236.

Kumar, S., Kumar, R., & Gandhi, K. S. (1991). Alternative mechanisms of drop breakage in stirred vessels. *Chemical Engineering Science*, *46*, 2483–2489.

Kumar, S., & Ramkrishna, D. (1996a). On the solution of population balance equations by discretization — I. A fixed pivot technique. *Chemical Engineering Science*, *51*, 1311–1332.

Kumar, S., & Ramkrishna, D. (1996b). On the solution of population balance equations by discretization — II. A moving pivot technique. *Chemical Engineering Science*, *51*, 1333–1342.

Luo, H., & Svendsen, H. F. (1996). Theoretical model for drop and bubble breakup in turbulent dispersions. *A.I.Ch.E. Journal*, *42*, 1225–1233.

Maggioris, D., Goulas, A., Alexopoulos, A. H., Chatzi, E. G., & Kiparissides, C. (1998). Use of CFD in prediction of particle size distribution in suspension polymer reactors. *Computers and Chemical Engineering*, *22* (Suppl.), S315–S322.

Pacek, A. W., Man, C. C., & Nienow, A. W. (1998). On the Sauter mean diameter and size distributions in turbulent liquid/liquid dispersions in a stirred vessel. *Chemical Engineering Science*, *53*, 2005–2011.

Pal, R. (1996). Effect of droplet size on the rheology of emulsions. *A.I.Ch.E. Journal*, *42*, 3181–3190.

Park, J. Y., & Blair, L. M. (1975). The effect of coalescence on drop size distribution in an agitated liquid-liquid dispersion. *Chemical Engineering Science*, *30*, 1057–1064.

Perry, R. H., & Green, D. W. (1997). Perry's chemical engineers' handbook (7th ed.). New York: McGraw-Hill.

Press, W. H., Teukolsky, S. A., Vetterling, W. T., & Flannery, B. P. (1993). *Numerical recipes in fortran* (2nd ed.). Cambridge: Cambridge University Press.

Schwartzberg, H. G., & Treybal, R. E. (1968). Fluid and particle motion in turbulent stirred tanks. *Industrial and Engineering Chemistry, Fundamentals*, 7, 1–6; 6–12.

Taylor, R., & Krishna, R. (1993). *Multicomponent mass transfer*. New York: Wiley.

Tsouris, C., & Tavlarides, L. L. (1994). Breakage and coalescence models for drops in turbulent dispersions. *A.I.Ch.E. Journal*, *40*, 395–406.

Valentas, K. J., & Amundson, N. R. (1966). Breakage and coalescence in dispersed phase systems. *Industrial and Engineering Chemistry, Fundamentals*, *5*, 533–542.

Vermeulen, T., Williams, G. M., & Langlois, G. E. (1955). Interfacial area in liquid-liquid and gas-liquid agitation. *Chemical Engineering Progress*, *51*, s. 85-F–94-F.

Wichterle, K. (1995). Drop breakup by impellers. *Chemical Engineering Science*, *50*, 3581–3586.

Zhou, G., & Kresta, S. M. (1998). Correlation of mean drop size and minimum drop size with turbulence energy dissipation and the flow in an agitated tank. *Chemical Engineering Science*, *53*, 2063–2079.